Dynamics of Atmospheres and Oceans 51 (2011) 137–150

Contents lists available at ScienceDirect

Dynamics of Atmospheres and Oceans

journal homepage: www.elsevier.com/locate/dynatmoce

Evaluation of turbulent Prandtl (Schmidt) number parameterizations for stably stratified environmental flows

Zachary A. Elliott, Subhas K. Venayagamoorthy*

Department of Civil and Environmental Engineering, Colorado State University, 1372 Campus Delivery, Fort Collins, CO 80523-1372, USA

ARTICLE INFO

Article history:
Received 1 September 2010
Received in revised form 21 February 2011
Accepted 28 February 2011
Available online 5 March 2011

Keywords:
Turbulence
Stable stratification
Turbulent Prandtl number
Mixing
Numerical modeling
Scalar flux

ABSTRACT

In this study, we evaluate four different parameterizations of the turbulent Prandtl (Schmidt) number $Pr_t = \nu_t/\Gamma_t$ where ν_t is the eddy viscosity and Γ_t is the scalar eddy diffusivity, for stably stratified flows. All four formulations of Pr_t are strictly functions of the gradient Richardson number *Ri*, which provides a measure of the strength of the stratification. A zero-equation (i.e. no extra transport equations are required) turbulence model for ν_t in a one-dimensional, turbulent channel flow is considered to evaluate the behavior of the different formulations of Pr_t. Both uni-directional and oscillatory flows are considered to simulate conditions representative of practical flow problems such as atmospheric boundary layer flows and tidally driven estuarine flows, to quantify the behavior of each of the four formulations of Pr_t. We perform model-to-model comparisons to highlight which of the models of Pr_t allow for a higher rate of turbulent mixing and which models significantly inhibit turbulent mixing in the presence of buoyancy forces resulting from linear (continuous) stratification as well as two-layer stratification. The basis underlying the formulation of each model in conjunction with the simulation results are used to emphasize the considerable variability in the different formulations and the importance of choosing an appropriate parameterization of Pr_t given a model for ν_t in stably stratified flows.

* Corresponding author. Tel.: +1 970 491 1915; fax: +1 970 491 7727.
E-mail addresses: zachary.elliott@rams.colostate.edu (Z.A. Elliott), vskaran@colostate.edu (S.K. Venayagamoorthy).

0377-0265/$ – see front matter © 2011 Elsevier B.V. All rights reserved.
doi:10.1016/j.dynatmoce.2011.02.003

1. Introduction

Stable density stratification is a common feature in environmental flows such as rivers, lakes, reservoirs, estuaries, oceans, and the atmospheric boundary layer. Stable stratification is characterized by a density gradient in which the density of the fluid increases with depth in a river, lake, or ocean or decreases with altitude in the atmosphere. This stable stratification can occur continually or can be marked by a denser fluid layer (e.g. salt water from the ocean) flowing beneath a less dense fluid layer (e.g. fresh water from a river) separated by a distinct interface. The interface of these two layers forms a sharp density gradient within the flow, often referred to as a pycnocline or thermocline. In either case, stable stratification tends to suppress turbulence; the buoyancy flux term in the governing equation for the turbulent kinetic energy of a flow acts as an energy sink in the presence of stable stratification to inhibit vertical mixing and dispersion from the turbulence generated from shear stress at the bottom boundary. As a result, turbulent properties of the flow that describe the vertical mixing and diffusion of momentum and scalars called the eddy viscosity and scalar eddy diffusivity respectively, are significantly affected, especially away from boundaries where turbulence is generated. Buoyancy effects become dominant in the interior part of the flow and mixing generated by the shear at the boundary is almost entirely suppressed across a sharp interface bounding one or more well mixed layers (Turner, 1973). Essentially, stable stratification and turbulence compete with one another to determine the rate and efficiency of vertical turbulent mixing in the flow. Excellent reviews of stably stratified environmental flows are given by Gregg (1987), Fernando (1991), Riley and Lelong (2000), Peltier and Caulfield (2003) and Ivey et al. (2008).

Predicting the vertical mixing and dispersion of a passive scalar, such as the concentration of a pollutant released at some depth within a stably stratified environmental flow, can be achieved by numerically solving the equations that govern the motion and properties of the flow. The equations that govern the behavior of a fluid are the well-known Navier–Stokes equations for conservation of momentum and the continuity equation for conservation of mass. However, it is not feasible in most cases to solve the highly nonlinear set of Navier–Stokes equations in their full form using direct numerical simulations (DNS) or large-eddy simulations (LES) due mainly to computational and geometrical constraints (see e.g. Ferziger and Peric, 2002 for a detailed discussion). A practical approach commonly used in engineering to obtain approximate (statistical) solutions to the Navier–Stokes equations is to use the Reynolds decomposition to cast them in terms of time-averaged variables by splitting each instantaneous variable into a mean component and a fluctuating component. This averaging process yields the so called Reynolds-averaged Navier–Stokes (RANS) equations and results in six additional terms called the Reynolds stresses in the averaged momentum equations and a turbulent scalar flux term in the scalar (density) transport equation. These turbulent flux terms give rise to what is commonly known as the closure problem in turbulent flows and hence necessitate the need for additional equations/models to close the system of equations (i.e. have enough equations to solve for each of the unknowns) in order to obtain solutions.

There are different computational methods for closing the RANS system of mean flow equations known as turbulence models, many of which rely on the turbulent Prandtl number $Pr_t = \nu_t/\Gamma_t$ to link the scalar eddy diffusivity Γ_t and the eddy viscosity ν_t (Venayagamoorthy and Stretch, 2010). Turbulence models may vary in complexity and completeness; for example a more complete method, which is more computationally expensive, is to solve six transport equations for each of the Reynolds stresses. However, a common approach is to use the Boussinesq turbulent-viscosity hypothesis to model the Reynolds stresses $\overline{u'w'}$ (for the simple case of a statistically one-dimensional flow) as a linear function of the mean shear rate $S = d\bar{u}/dz$ multiplied by ν_t. Again, there are different approaches to modeling ν_t ranging from more complete two-equation turbulence models to simplified zero-equation algebraic models. Two-equation turbulence models such as the k–ε model describe ν_t as a function of the turbulent kinetic energy k and the turbulent kinetic energy dissipation rate ε, which are in turn given by two partial differential equations that must be solved within the framework of the RANS equations. Zero-equation models are the simplest turbulence models that use algebraic expressions for the eddy viscosity and hence do not require the solution of any additional partial differential equation (Chen and Jaw, 1998; Ferziger and Peric, 2002). They are therefore easy to implement and can often yield accurate and insightful results for certain (simple) types of turbulent flows.

The objectives of this paper are to investigate the effects of stable stratification on the vertical turbulent mixing of a passive scalar using four different formulations of the turbulent Prandtl (Schmidt) number Pr_t and to evaluate their performance for use in turbulence models that may apply to rivers, lakes, estuaries, oceans, and the atmosphere. In Section 2, the theoretical background for density stratification and its effect on the eddy viscosity model used in this study are presented. In Section 3, we outline the model setup and present the governing equations, numerical methodology, and parameters of interest in the numerical model used to obtain results for each of the formulations of Pr_t. In Section 4, the four different formulations of Pr_t used in this study are presented along with the underlying basis of their formulations. The results and discussion are presented in Section 5 and conclusions are given in Section 6.

2. Theoretical background

The results of the present study focus primarily on the relationship between Pr_t and the strength of stratification of the flow as characterized by the gradient Richardson number $Ri = N^2/S^2$, where $N = \sqrt{(-g/\rho_0)(d\bar{\rho}/dz)}$ is the Brunt–Väisälä (or buoyancy) frequency. Thus, a simple zero-equation turbulence model for shallow flows in an equilibrium state of turbulence was used to represent ν_t. Assuming a one-dimensional, fully developed turbulent channel flow with a hydrostatic pressure distribution and a logarithmic velocity profile, a parabolic eddy viscosity model for ν_t as a function of the flow depth z can be derived for a neutrally stable case by using a momentum balance between the horizontal pressure gradient and turbulent shear stress (vertical mixing) in conjunction with the Boussinesq turbulent-viscosity hypothesis as (Rodi, 1993)

$$\nu_t(z) = \kappa u_\tau \left(\frac{-z}{H}\right)(H+z), \tag{1}$$

where κ is the von Karman constant (taken as $\kappa = 0.41$), u_τ is the shear or friction velocity, H is the total flow depth in the channel, and $z = 0$ at the free surface. The simple parabolic eddy viscosity model given by Eq. (1) only accounts for turbulence generated at the bottom boundary of the channel by the bed friction, but can still be effectively used for fully developed channel flows.

Because stable stratification in the channel can significantly limit the vertical turbulent mixing away from the channel bed, the parabolic eddy viscosity model given in Eq. (1) can be modified in the presence of stable stratification according to a model proposed by Munk and Anderson (1948). Their algebraic model for the modified eddy viscosity $\nu_t|_{\text{mod}}$ accounts for the vertical effect of the buoyancy forces caused by stable stratification by describing $\nu_t|_{\text{mod}}$ as a function of Ri and the flow depth z as

$$\nu_t|_{\text{mod}}(z) = \nu_t(1+\beta Ri)^\alpha, \tag{2}$$

where β and α are experimentally determined constants with given values of 10 and $-1/2$, respectively (Munk and Anderson, 1948). It is clear that the value of $\nu_t|_{\text{mod}}$ is significantly reduced where there is a strong density gradient in the flow limiting the turbulent mixing. However, Munk and Anderson's model given by Eq. (2) does not account for the suppression of turbulence generated at the channel bed in fluid layers above a pycnocline in the case of two-layer stratification where the density may again become relatively constant up to the free surface. Thus, it is not reasonable to let the eddy viscosity be unaffected above the pycnocline since the only source of turbulence is assumed to be from the bottom shear stress. Therefore in the presence of a pycnocline, it is reasonable to further adapt the model for $\nu_t|_{\text{mod}}$ by limiting the eddy viscosity above the pycnocline to a cut-off value less than the value of $\nu_t|_{\text{mod}}$ computed at the mid-depth of the pycnocline from Eq. (2). Above the pycnocline then, $\nu_t|_{\text{mod}}$ is modeled as a parabolic function, decreasing from the value of $\nu_t|_{\text{mod}}$ computed at the mid-depth of the pycnocline to zero at the free surface (personal communication, Robert L. Street). This is given by

$$\nu_t|_{\text{mod}}(z) = \nu_t|_{\text{mod},pyc}\left(\frac{z}{z_{pyc}}\right)\left(2-\frac{z}{z_{pyc}}\right) \quad \text{for } z > z_{pyc}, \tag{3}$$

where z_{pyc} is the mid-depth of the pycnocline and $\nu_t|_{\text{mod},pyc}$ is the value of $\nu_t|_{\text{mod}}$ computed at the mid-depth of the pycnocline from Eq. (2). This approach, designated as the modified Munk and Anderson (1948) cut-off model, is admittedly simple but it mimics the suppression of turbulent mixing generated

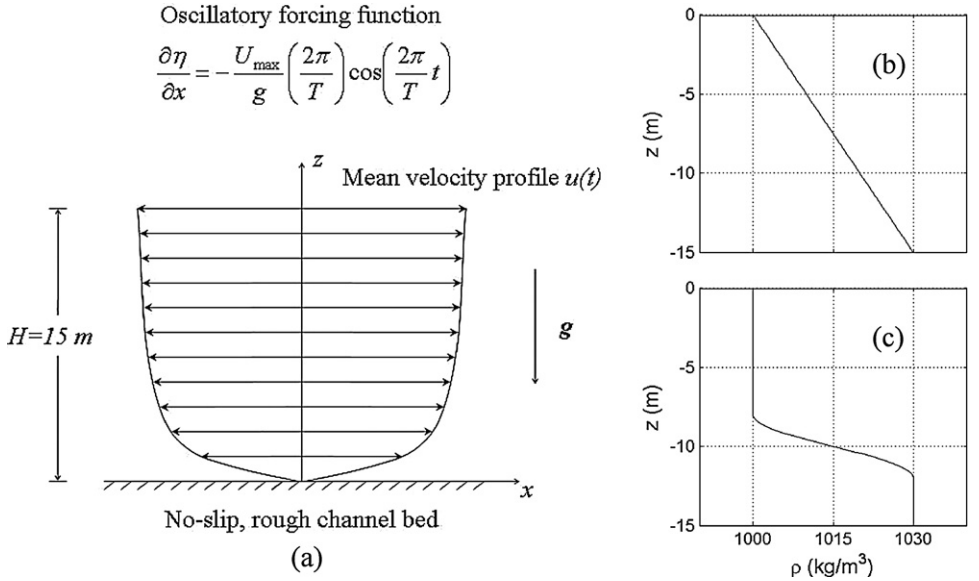

Fig. 1. Schematic of the problem set-up depicting (a) the tidal velocity field; (b) a continuous stratification density profile; and (c) a two-layered stratification density profile.

at the channel bed above the sharp density gradient while still modeling $\nu_t|_{\mathrm{mod}}$ as a parabolic shape as derived in Eq. (1).

3. Numerical model set-up

Accepting the modified Munk and Anderson (1948) formulation as a model for the eddy viscosity ν_t, different formulations of Pr_t and its effect on the scalar eddy diffusivity Γ_t and mixing of a passive scalar in stably stratified flows were then investigated by simulating a simple one-dimensional channel flow. The flow was assumed to be fully developed and one-dimensional such that the flow variables are horizontally homogeneous and characterized by either a constant, continuous vertical density gradient or a sharp density gradient interface separating two fluid layers of relatively constant density akin to flow in a coastal estuary channel or an atmospheric boundary layer as shown in the schematic in Fig. 1. A somewhat artificial test case was used in that the density profile was held fixed in time, in some ways similar to the simulations and experiments done by Venayagamoorthy et al. (2003) and Komori et al. (1983). Hence, the calculations assume that the density profile is unchanged by the turbulent mixing that occurs, illustrating a situation where the stratification is very strong and/or that the mixing takes place in much shorter timescales than the effect of turbulence on the stratification. For this simple one-dimensional flow, the horizontal terms can be ignored since the balance is primarily between the pressure gradient and vertical turbulent mixing. Hence, the governing equations are a form of the horizontal momentum equation coupled with a prescribed forcing equation that can be used as a periodic function to model the effect of the ebb and flow of a tide in an estuary. These equations are given respectively as

$$\frac{\partial u}{\partial t} = -g\frac{\partial \eta}{\partial x} + \frac{\partial}{\partial z}\left[\nu_t|_{\mathrm{mod}}\frac{\partial u}{\partial z}\right], \tag{4}$$

and

$$\frac{\partial \eta}{\partial x} = -\frac{U_{\max}}{g}\left(\frac{2\pi}{T}\right)\cos\left(\frac{2\pi}{T}t\right), \tag{5}$$

where u is the streamwise velocity, η is the free surface elevation, g is the acceleration due to gravity (taken as $g = 9.81\ \mathrm{m/s^2}$), T is the period of the semi-diurnal tide (i.e. 12.42 h for a M_2 tidal constituent), and $U_{\max}$ is a prescribed maximum velocity of the flow in the channel. The scalar diffusion equation used to model the change in concentration of a passive scalar C over the depth of the channel in time is given by

$$\frac{\partial C}{\partial t} = \frac{\partial}{\partial z}\left[\Gamma_t \frac{\partial C}{\partial z}\right], \tag{6}$$

where Γ_t is the scalar eddy diffusivity computed from the modified Munk and Anderson (1948) formulation of the eddy viscosity and a given formulation of Pr_t as a function of Ri.

The governing partial differential equations given in Eqs. (4)–(6) are more amenable to numerical solutions than analytical solutions since the eddy viscosity depends on Ri, which can vary with depth over a wide range of values. Eqs. (4)–(6) must therefore be discretized in space and time to obtain solutions. The accuracy of the discretization scheme chosen is based on the order of the terms that are retained from a Taylor series expansion of the derivative terms. For this model, a second-order accurate, central-differencing scheme based on a finite volume formulation was used to approximate the spatial derivatives. A semi-implicit discretization scheme known as the θ-method was used to approximate the temporal derivatives of the governing equations. The θ-method makes use of the implicitness parameter θ to improve the accuracy and efficiency of the scheme (Casulli and Cattani, 1994). The objective of the θ-method is to give more or less weighting to the implicit terms in the discretized equation, or the unknown terms being evaluated for the next time step $n+1$ in the time-marching solution algorithm. This weighting of implicit terms is based on the value of θ, which can range anywhere from 0 to 1. If $\theta = 0$, then the scheme is fully explicit and first-order accurate in time and there are no implicit terms to be solved for in the equation. Conversely, if $\theta = 1$, then the scheme is fully implicit and first-order accurate in time and there is no weight given to the explicit terms. However, if θ takes a value between 0 and 1, the scheme becomes semi-implicit and between first- and second-order accurate in time. When $\theta = 0.5$, variables in the governing equations are evaluated as an average of their values at time levels n and $n+1$ so that the discretization is second-order accurate in time (known as the Crank–Nicolson scheme). The method has been shown to be stable for $0.5 \leq \theta \leq 1$, with second-order time accuracy for $\theta = 0.5$. When $\theta < 0.5$, the method is only conditionally stable (Casulli and Cattani, 1994). It has been shown that a value of θ slightly greater than 0.5 can be used in order to dampen and eliminate high-frequency oscillations (i.e. obtain asymptotic stability) without adversely affecting the simulations with numerically induced diffusion (Fringer et al., 2006). It was found for this problem that a value of $\theta \approx 0.7$ produced oscillation-free solutions.

In order to completely define and be able to solve the set of discretized equations, initial and boundary conditions must be defined to start the solution algorithm and relate it to the system in which it is being analyzed. To initialize the velocity field of the flow at some starting point in time for the uni-directional channel flow, the model was spun-up and the flow was allowed to reach a fully developed turbulent velocity profile before the passive scalar C was released in the flow. For the case of the tidally driven channel flow, the velocity in the channel was set to zero and allowed to be initialized by the effect of the periodic tidal forcing function defined in (5). Consequently, the variation with depth of $\nu_t|_{\mathrm{mod}}$ in the channel, being a function of the shear velocity near the channel bed, is dictated by the prescribed initial velocity field of the flow. Flux (or Neumann) boundary conditions at the free surface and at the bed were specified to completely define the problem. At the free surface, wind shear was not considered and hence the velocity gradient in the vertical direction was assumed to be zero due to the expected behavior of the log-law velocity profile to reach a maximum value near the free surface. At the channel bed, the effects of a rough bed and a viscous boundary layer are given by the drag law to represent the shear stress at the boundary (Fringer et al., 2006). The velocity gradient in the vertical direction was modeled as a function of the drag coefficient C_D (which depends on the channel roughness), ν_t at the boundary, and the flow velocity near the boundary u_1 given as

$$\left.\frac{\partial u}{\partial z}\right|_{z=-H} = \frac{C_D}{\nu_t}\,|u_1|\,u_1, \tag{7}$$

where u_1 is the mean flow velocity at the first grid point from the lower boundary or bed of the channel. It is important to note that for real flows with rough boundaries a wall point to define the no-slip condition where the velocity goes to zero cannot be consistently defined due to the irregular roughness elements of the channel bed. Therefore, the boundary condition was applied some distance away from the actual boundary to account for the roughness elements of a real channel. The maximum velocity in the channel $U_{\max}$ was prescribed for each case such that the maximum value of $\nu_t|_{\mathrm{mod}}$ reached in the channel was the same for both the uni-directional channel flow case and the oscillatory channel flow case. This corresponds approximately to a friction Reynolds number of $Re_\tau = u_\tau H/\nu = 273{,}300$ and a friction Richardson number $Ri_\tau = (NH/u_\tau)^2 = 13{,}300$ for the continuously stratified uni-directional flow simulations and $Re_\tau = 386{,}000$ and $Ri_\tau = 6670$ for the two-layered stratified uni-directional flow simulations. $Re_\tau = 335{,}000$ and $Ri_\tau = 8880$ for the continuously stratified oscillatory case (based on the maximum value of u_τ reached at the peak of the ebb or flood cycle) and $Re_\tau = 367{,}000$ and $Ri_\tau = 7360$ for the two-layered stratified oscillatory flow case.

The parameters of interest in the problem including the variation in density and initial concentration and distribution of the passive scalar C must also be specified as functions of space and time. As prescribed, the flow was modeled as a stably stratified flow as either a constant, continuous density gradient or as a distinct, sharp gradient between two layers of fluids of relatively constant density as shown in Fig. 1(b) and (c), respectively. The position of the distinct pycnocline interface between the two densities can be clearly seen in Fig. 1(c). Also, the initial distribution and position of a passive scalar C was centered at three different depths in the channel for each of the two density stratifications, above the position of the pycnocline, at the position of the pycnocline, and below the position of the pycnocline as shown in Figs. 4(a)–(c) and 5(a)–(c), respectively.

With the complete set of discretized equations, initial conditions, and boundary conditions defined, a solution algorithm was developed and programmed to march the solution forward in time. Since the algorithm uses a semi-implicit time discretization scheme, the matrix of discretized equations at each grid point varying with depth in the channel must be solved simultaneously at each time step to produce a solution. To program this, a time-marching loop was coded into the algorithm to update the coefficients ($\nu_t|_{\mathrm{mod}}$ and Ri) at each time step so that the implicit matrix equations for velocity and concentration at the next time step could be solved. Due to the one-dimensional nature of the problem, the linear system of equations yields a tri-diagonal matrix system which can be easily solved using a sparse Gaussian elimination procedure such as the Thomas Algorithm. All coding and output of model results was done in MATLAB (R2009, the Mathworks, Inc., Natick, MA, USA).

4. Turbulent Prandtl number formulations

Four different formulations of Pr_t as a function of Ri were considered to study the effects of stratification on Γ_t as well as the vertical mixing of C in Eq. (6) given the zero-equation eddy viscosity model in Eq. (2) proposed by Munk and Anderson (1948) for the case of the linear stratification and the modified cut-off Munk and Anderson model for the two-layered stratification. A key debate in the stratified modeling community pertains to the issue of whether turbulence is completely quenched at high values of Ri (Galperin et al., 2007). There are a number of models for Pr_t ranging from those that propose an asymptotic maximum value for Pr_t beyond a critical value of Ri based on the concept of turbulence extinction to formulations where Pr_t continues to increase monotonically as a function of Ri. Three of the four formulations chosen for this study are based on the concept that scalar mixing is inhibited in an ever increasing manner as functions of Ri without any asymptotic leveling off of mixing. Each of the formulations of Pr_t was tested for both the continuously stratified case and the two-layered stratified case in a uni-directional flow as well as a tidally driven oscillatory flow.

The first expression of Pr_t considered is also a formulation by Munk and Anderson (1948) (hereafter MA). They proposed a model for a modified scalar eddy diffusivity $\Gamma_t|_{\mathrm{mod}}$ of the same form as $\nu_t|_{\mathrm{mod}}$ in Eq. (2) to account for the effect of buoyant forces given as

$$\Gamma_t|_{\mathrm{mod}}(z) = \Gamma_t(1 + \beta_\rho Ri)^{\alpha_\rho}, \tag{8}$$

where β_ρ and α_ρ are again empirical constants with prescribed values of 10/3 and −3/2 respectively (Munk and Anderson, 1948). Pr_t as a function of Ri is obtained by dividing Eq. (2) by Eq. (8) to get

$$Pr_t = \frac{\nu_t}{\Gamma_t}\frac{(1+\beta Ri)^\alpha}{(1+\beta_\rho Ri)^{\alpha_\rho}}, \tag{9}$$

where ν_t/Γ_t can be defined as the turbulent Prandtl number for the neutrally stratified case Pr_{t0} such that Eq. (9) can be rewritten as

$$Pr_t = Pr_{t0}\frac{(1+\beta Ri)^\alpha}{(1+\beta_\rho Ri)^{\alpha_\rho}}, \tag{10}$$

The second relationship for Pr_t based on Ri was recently derived by Venayagamoorthy and Stretch (2010) (hereafter VS) using theoretical arguments supported by DNS data for homogeneous stably stratified turbulent flows. Their model for Pr_t as a function of Ri is given as

$$Pr_t = Pr_{t0}\exp\left(-\frac{Ri}{Pr_{t0}\Gamma_\infty}\right) + \frac{Ri}{R_{f\infty}}, \tag{11}$$

where Γ_∞ is the mixing efficiency and $R_{f\infty}$ is the asymptotic value of the flux Richardson number. The DNS results analyzed by VS indicate an average value of $\Gamma_\infty \approx 1/3$, which translates to $R_{f\infty} \approx 1/4$ since these two quantities are related by $\Gamma_\infty = R_{f\infty}/(1-R_{f\infty})$ (Venayagamoorthy and Stretch, 2010).

There has been much work and research done concerning the value of Pr_{t0} in neutrally stratified flows. Data from numerical simulations and experiments done by Kays and Crawford (1993) and Kays (1994) suggest values of Pr_{t0} between 0.5 and 1.0 for neutrally stratified flows. Theoretical reasoning and DNS data analyzed by VS further suggest that Pr_{t0} is approximately equal to the ratio of the scalar timescale T_ρ to the mechanical (turbulence) timescale T_L or $Pr_{t0} \approx 1/(2\gamma)$ where $\gamma = (1/2)(T_L/T_\rho)$. Using $\gamma \approx 0.7$ as suggested by Venayagamoorthy and Stretch (2006) yields a value of $Pr_{t0} \approx 0.7$. This neutral value of the turbulent Prandtl number has been adopted for the present study.

The third formulation for Pr_t is given by Kim and Mahrt (1992) (hereafter KM). Their formulation of Pr_t is derived from the Louis model that relates the mixing length for heat to the Richardson number (Louis, 1979; Louis et al., 1981). Using aircraft data to validate their model, KM arrive at a formulation of Pr_t similar to that of MA as

$$Pr_t = Pr_{t0}\frac{1+15Ri(1+5Ri)^{1/2}}{1+10Ri(1+5Ri)^{-1/2}}. \tag{12}$$

The final formulation of Pr_t is derived from expressions of ν_t and Γ_t presented by Strang and Fernando (2001) from formulations by Peters et al. (1988) (hereafter PGT). The PGT empirical formulations of the eddy viscosity and scalar eddy diffusivity are driven by data obtained from a study of the Pacific Ocean near the equator (Peters et al., 1988) and given respectively as

$$\nu_t = 5.6\times 10^{-4}\cdot Ri^{-8.2} \tag{13}$$

and

$$\Gamma_t = 3.0\times 10^{-5}\cdot Ri^{-9.6} \tag{14}$$

for $Ri \le 0.25$ and as

$$\nu_t = \frac{5.0}{(1.0+5.0Ri)^{1.5}} + 0.2 \tag{15}$$

and

$$\Gamma_t = \frac{5.0}{(1.0+5.0Ri)^{2.5}} + 0.01 \tag{16}$$

for $Ri > 0.25$ (Strang and Fernando, 2001). Combining Eqs. (13) and (14) for $Ri \le 0.25$ and Eqs. (15) and (16) for $Ri > 0.25$ respectively yields a model for Pr_t as

$$Pr_t = \frac{56}{3}Ri^{1.4} \quad \text{for } Ri \le 0.25 \tag{17}$$

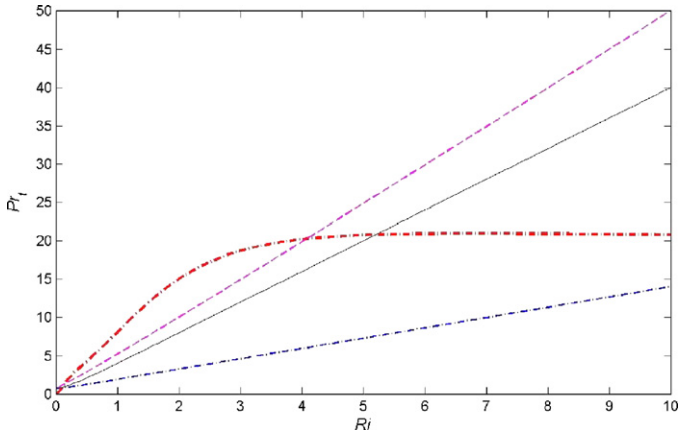

Fig. 2. The turbulent Prandtl number Pr_t as a function of the gradient Richardson number Ri for four different models: blue dashed-dotted line, Munk and Anderson (1948); black solid line, Venayagamoorthy and Stretch (2010); purple dashed line, Kim and Mahrt (1992); red thick dashed-dotted line, Peters et al. (1988). (For interpretation of the references to color in this figure legend, the reader is referred to the web version of the article.)

and

$$Pr_t = \frac{5.0(1.0 + 5.0Ri)^{-1.5} + 0.2}{5.0(1.0 + 5.0Ri)^{-2.5} + 0.01} \quad \text{for } Ri > 0.25. \tag{18}$$

This model of Pr_t proposed by PGT behaves differently from the other three models in that here Pr_t does not continue to grow with increasing Ri. Instead, it asymptotically approaches a maximum value of $Pr_t \approx 20$ as $Ri \to \infty$ (see Fig. 2). Also, it is important to note that this empirical formulation of Pr_t yields a value of 0 when $Ri = 0$ (i.e. unstratified flow). This would imply that there is infinite turbulent mixing of a passive scalar for neutrally stratified flows. This clearly implies that this model would only be physically applicable for $Ri > 0$ (i.e. stratified flow) as opposed to the other three formulations, which are more general in that there is a seamless transition to the unstratified case with $Pr_t \to Pr_{t0}$ as $Ri \to 0$. Each of the four functions of Pr_t considered in this study are shown as a function of Ri in Fig. 2 with the upper bound value of Ri truncated at 10 for clarity.

It might appear to be obvious from Fig. 2 as to which of these models will permit greater levels of mixing or vice versa. Clearly KM has the steepest slope implying less scalar mixing while MA has the smallest slope indicating enhanced scalar mixing. However, the model by PGT suggests a much stronger suppression of scalar mixing for lower values of Ri than the rest but higher levels of mixing compared to KM for $Ri > 4.1$, VS for $Ri > 5.2$, and MA for $Ri > 14.9$. Given the large range of values of Ri that varies with flow depth in a channel flow (for a nice theoretical discussion, see Armenio and Sarkar, 2002), the mixing properties of each of the Pr_t formulations might not be immediately apparent and only through test cases like those discussed in the next section can they be best understood.

5. Results

All four of the Pr_t formulations were tested for the two types of stratified flow conditions shown in Fig. 1(b) and (c) for three different locations of an initial passive scalar plume C as depicted in Figs. 4(a)–(c) and 5(a)–(c), respectively. All of these cases were tested for a fully developed uni-directional stratified channel flow and for a tidally driven stratified channel flow in which the velocity field changes as a function of time. The results of the stably stratified flows were then compared to a base case of an unstratified flow, which is shown in Fig. 3. The unstratified cases were tested first and the model was run until the initial plume was completely mixed over the depth of the channel (see Fig. 3(c)). This took approximately 5800 s for both cases (approximately 0.13 M_2 tidal periods). The mixing of C from its initial condition for the two-layered stratified and continuously stratified cases

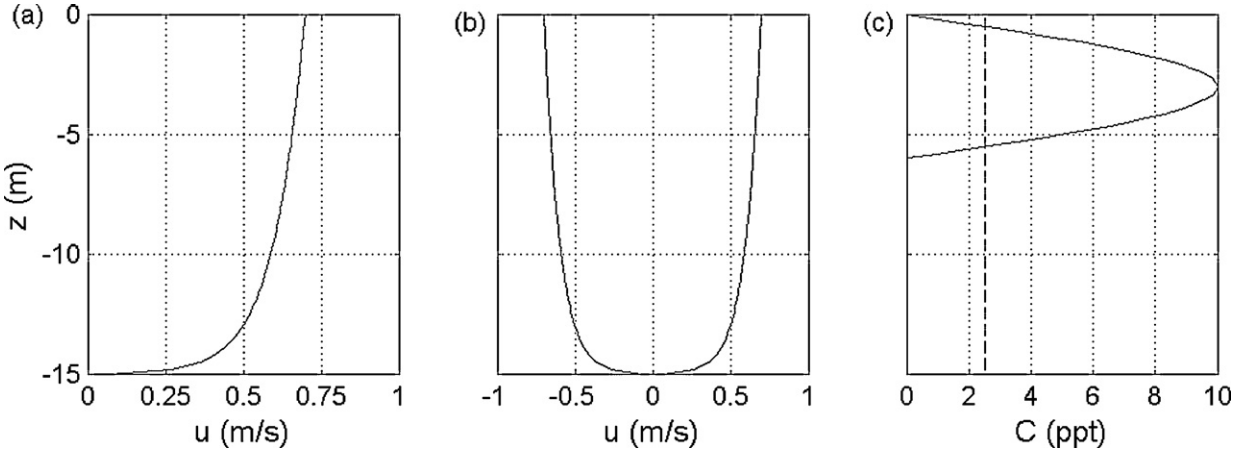

Fig. 3. Fully developed velocity profiles and concentration profiles for the unstratified base case, (a) uni-directional flow; (b) oscillatory flow; and (c) initial concentration profile: solid line, and final concentration profile: dashed line.

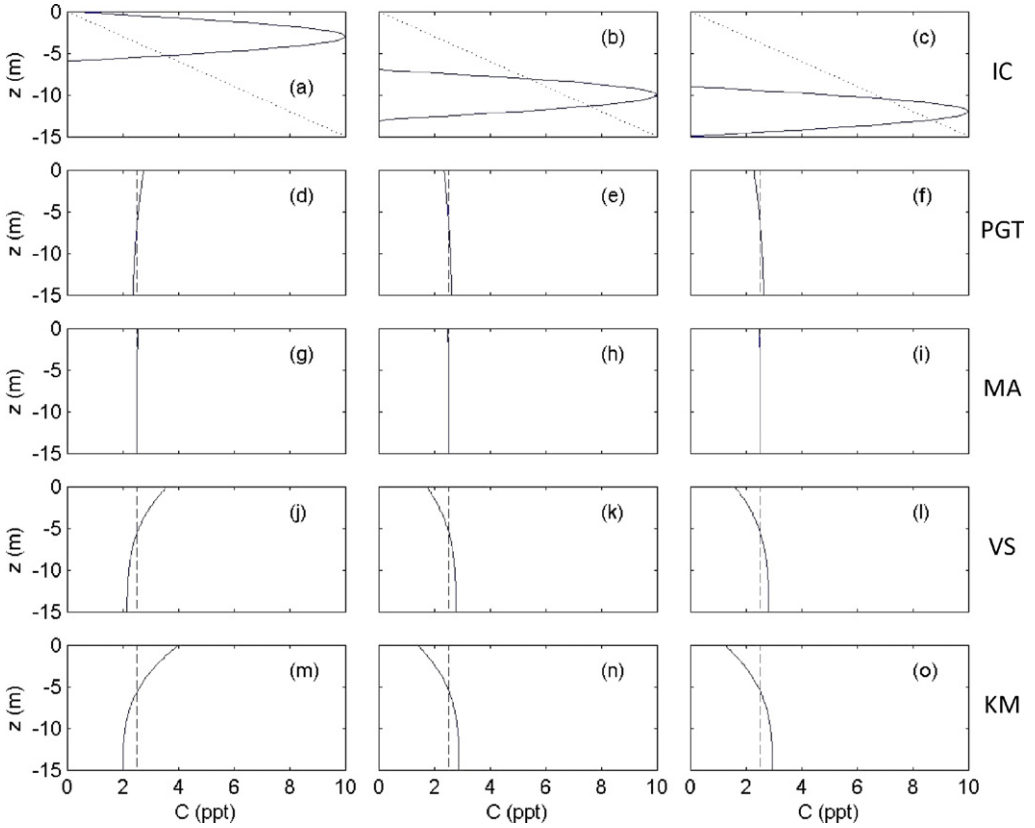

Fig. 4. Concentration profiles for a passive scalar C in a continuously stratified uni-directional channel flow. Subplots (a)–(c) show the initial conditions (IC) of the passive scalar plume. Final concentration profiles are shown in subplots (d)–(f) using the PGT model; subplots (g)–(i) using the MA model; subplots (j)–(l) using the VS model; and subplots (m)–(o) using the KM model, respectively. Also superimposed on subplots (d)–(o) is the final profile for the unstratified case.

required a period of approximately 50 ($\approx$6.5 M_2 tidal periods) and 100 ($\approx$13 M_2 tidal periods) times the time that was required for the unstratified case to mix out. A total of 18 simulations runs were performed to assess these four Pr_t models.

Fig. 4 shows the concentration distributions of C for the continuously stratified case in a uni-directional channel flow. The initial passive scalar plume C with a maximum concentration of 10 ppt was released near the top (free surface), near the middle, and close to the bed of the channel in a fully developed channel flow as shown in Fig. 4(a)–(c). For each of the three different cases, each of the four formulations of Pr_t was implemented to predict the vertical mixing of C. For this case, the MA model predicted the maximum amount of turbulent mixing of C (see Fig. 4(g)–(i)) while the KM model predicted the minimum amount of turbulent mixing of C as shown in Fig. 4(m)–(o). The final concentration profiles for the PGT model are shown in Fig. 4(d)–(f) and those for the VS model are given in Fig. 4(j)–(l). The Ri values close to the free surface get quite large for this linearly stratified case and hence the models of both VS and KM predict the least amount of scalar mixing as can be seen from the concentration gradients at the free surface in Fig. 4(j)–(l) and (m)–(o), respectively.

Fig. 5 shows the concentration distributions for the two-layered stratified case (with a pycnocline) in a uni-directional channel flow. Again, the passive scalar plume C with a maximum concentration of 10 ppt was released at the same three locations as for the continuously stratified case shown in Fig. 4. For this case, the MA model for Pr_t once again mixed out the initial plume the quickest over the depth of the channel as shown in Fig. 5(g)–(i). At the same corresponding time, the model of PGT had also

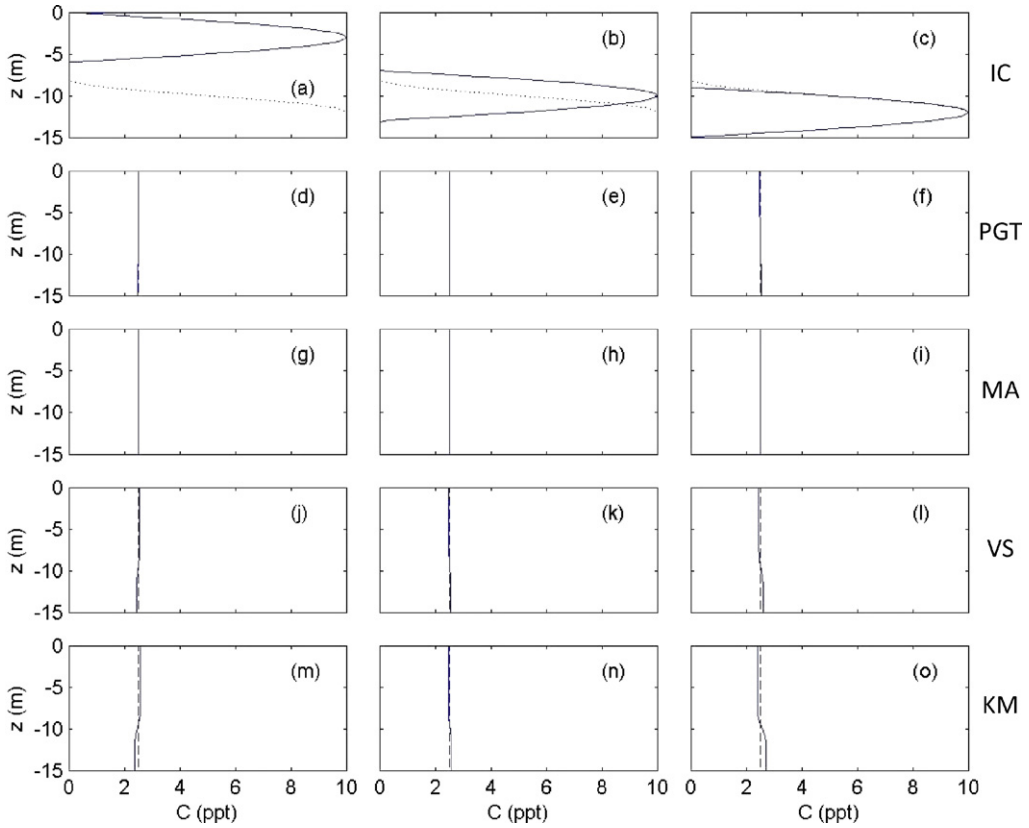

Fig. 5. Concentration profiles for a passive scalar C in a two-layered stratified uni-directional channel flow. Subplots (a)–(c) show the initial conditions (IC) of the passive scalar plume. Final concentration profiles are shown in subplots (d)–(f) using the PGT model; subplots (g)–(i) using the MA model; subplots (j)–(l) using the VS model; and subplots (m)–(o) using the KM model, respectively. Also superimposed on subplots (d)–(o) is the final profile for the unstratified case.

almost completely mixed out the initial profile as can be seen in Fig. 5(d)–(f). The final concentration profiles using the VS model are also almost completely mixed out and so were the final concentration profiles from the KM model, but the KM model predicted the least amount of mixing of C among the four models at the same corresponding time over the depth of the flow.

The same conditions and models were then tested for the case of a tidally driven periodic channel flow in which the velocity field changes direction as a function of time (see the velocity profile shown in Figs. 1(a) and 3(b)). For this oscillatory flow case, the turbulence grows and decays with the phase of the tide and hence stratification effects are expected to be more dominant for this flow condition compared with the uni-directional flow cases shown in Figs. 4 and 5.

Fig. 6 shows the results of the mixing of C for each of the four formulations of Pr_t for a continuously stratified tidally driven flow. Fig. 7 shows the results of the mixing of C for the two-layered stratified tidally driven flow. For both of these cases and for all three initial release locations of the plume, the PGT model predicted the quickest turbulent mixing of C as shown in Figs. 6(d)–(f) and 7(d)–(f) and the KM model again predicted the slowest turbulent mixing of C (see Figs. 6(m)–(o) and 7(m)–(o)). The final concentration profiles from the MA model shown in Figs. 6(g)–(i) and 7(g)–(i) are not quite as well mixed as the profiles from the PGT model for the oscillatory flow case. This is a direct result of the increased influence of buoyancy forces over a substantial portion of the flow depth with Ri values well above the cross-over value of $Ri = 14.9$ between these two models discussed earlier (see Fig. 2), especially for the linearly stratified case. The VS model continues to fall in between the extremes of

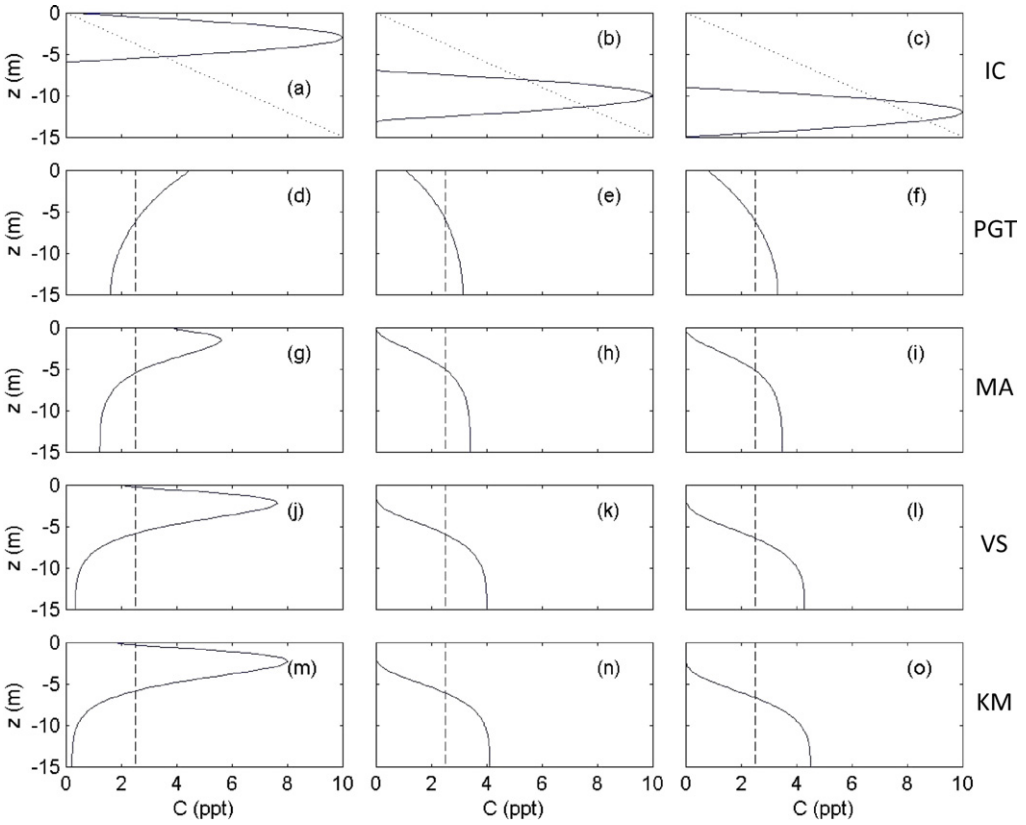

Fig. 6. Concentration profiles for a passive scalar C in a continuously stratified tidally driven channel flow. Subplots (a)–(c) show the initial conditions (IC) of the passive scalar plume. Final concentration profiles are shown in subplots (d)–(f) using the PGT model; subplots (g)–(i) using the MA model; subplots (j)–(l) using the VS model; and subplots (m)–(o) using the KM model, respectively. Also superimposed on subplots (d)–(o) is the final profile for the unstratified case.

high and low mixing as shown in Figs. 6(j)–(l) and 7(j)–(l), respectively. This is expected from the model behavior of Pr_t as a function of Ri as shown in Fig. 2.

6. Concluding remarks

In this study, we have used a one-dimensional vertical fluid column numerical model to evaluate and compare four different parameterizations of the turbulent Prandtl number Pr_t that are used in turbulence closure models. The four parameterizations of Pr_t that we have considered in this study are based on different hypotheses, observations and numerical simulations, and show considerable variability. For example, the formulation presented by VS is the only model considered here that is based on theoretical derivation and physical arguments supported by DNS data as opposed to the others which are mainly empirically driven. The results from model-to-model comparisons using simple turbulent open channel flow test cases highlight the effects of strong stratification in high Reynolds number flows and the impact of the different parameterizations of Pr_t on the vertical mixing of a passive scalar plume. The asymptotic behavior of Pr_t for large Ri in the PGT model allowed for a greater level of mixing than the other three models, especially for the strongly stratified oscillatory channel flow cases as shown in Figs. 6 and 7, respectively. On the other hand, the VS model always predicted a rate of mixing of C that was less than the models of PGT and MA, but had a mixing rate greater than the model proposed by KM. While model-to-model comparisons alone are not sufficient

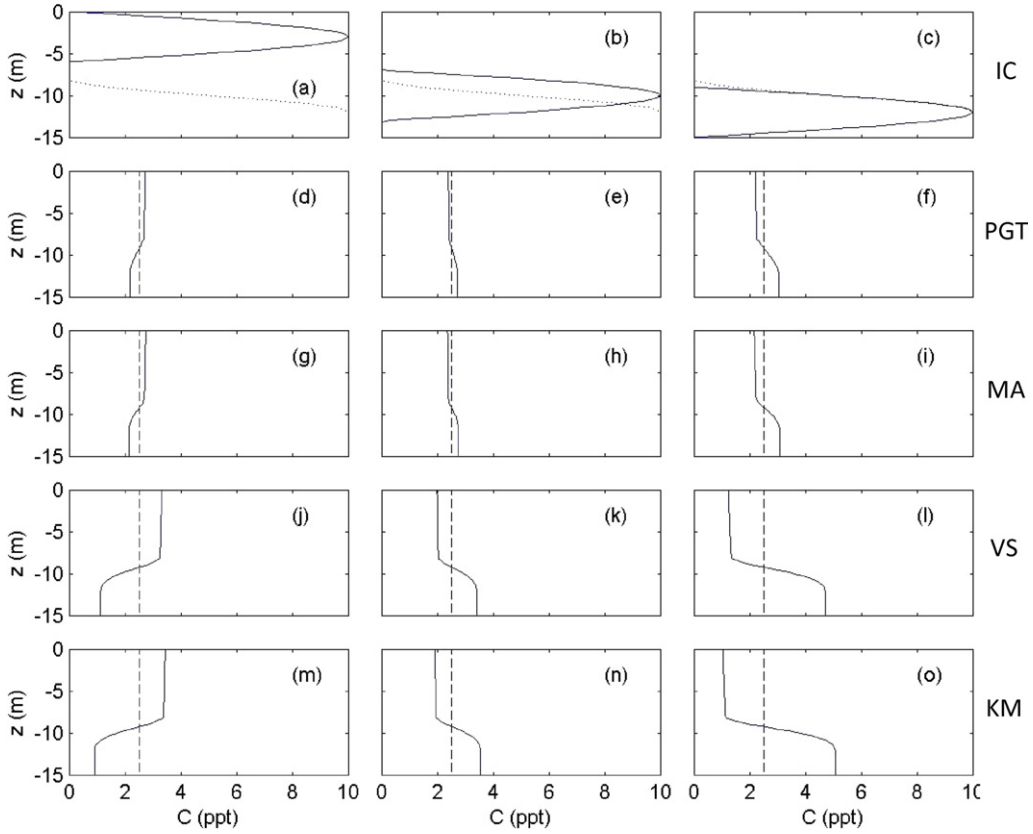

Fig. 7. Concentration profiles for a passive scalar C in a two-layered stratified tidally driven channel flow. Subplots (a)–(c) show the initial conditions (IC) of the passive scalar plume. Final concentration profiles are shown in subplots (d)–(f) using the PGT model; subplots (g)–(i) using the MA model; subplots (j)–(l) using the VS model; and subplots (m)–(o) using the KM model, respectively. Also superimposed on subplots (d)–(o) is the final profile for the unstratified case.

in pinpointing the most appropriate model for Pr_t, they nevertheless provide valuable insight on the performance of the different parameterizations under these simple but strong test cases for scalar mixing. Given that the VS model was the only model with strong theoretical underpinning, it appears to be a promising choice but its appropriateness remains to be validated with field measurements. Furthermore, it is worth noting that this study shows how even a one-dimensional vertical fluid column model with a zero-equation turbulence closure scheme can be used to highlight the effects of stable stratification on turbulence and vertical mixing of passive scalars.

A natural extension of this study is to include the effects of stratification more explicitly in the formulation of the turbulent eddy viscosity in RANS turbulence models. For example, the effect of the buoyancy parameter ($C_{\varepsilon 3}$) in the two-equation k–ε model (Launder and Spalding, 1972; Rodi, 1993) needs to be explored as a function of stratification in a similar vein to the earlier work by Venayagamoorthy et al. (2003). To this end, it is important to obtain data for strongly stratified and inhomogeneous flows to facilitate ongoing efforts to develop better turbulence models for stably stratified flows.

Acknowledgment

We thank the three anonymous reviewers for their constructive comments and recommendations which were very helpful in improving both the content and clarity of this paper. SKV wishes

to gratefully acknowledge Professor Robert Street for his enthusiasm and many insightful and interesting discussions on turbulence modeling at Stanford University. SKV also gratefully acknowledges the support of ONR grant N00014-10-1-0607 (Scientific officers: Dr Terri Paluszkiewicz and Dr Scott Harper).

References

Armenio, V., Sarkar, S., 2002. An investigation of stably stratified turbulent channel flow using large-eddy simulation. J. Fluid Mech. 459, 1–42.
Casulli, V., Cattani, E., 1994. Stability, accuracy and efficiency of a semi-implicit method for three-dimensional shallow water flow. Comput. Math. Appl. 27, 99–112.
Chen, C.-J., Jaw, S.-Y., 1998. Fundamentals of Turbulence Modeling. Taylor & Francis, New York.
Fernando, H.J.S., 1991. Mixing efficiency in stratified shear flows. Annu. Rev. Fluid Mech. 23, 455–493.
Ferziger, J.H., Peric, M., 2002. Computational Methods for Fluid Dynamics. Springer, Berlin.
Fringer, O.B., Gerritsen, M., Street, R.L., 2006. An unstructured-grid, finite-volume, nonhydrostatic, parallel coastal ocean simulator. Ocean Modell. 14, 139–173.
Galperin, B., Sukoriansky, S., Anderson, P.S., 2007. On the critical Richardson number in stably stratified turbulence. Atmos. Sci. Lett. 8, 65–69.
Gregg, M.C., 1987. Diapycnal mixing in the thermocline. J. Geophys. Res. 92, 5249–5286.
Ivey, G.N., Winters, K.B., Koseff, J.R., 2008. Density stratification, turbulence, but how much mixing? Annu. Rev. Fluid Mech. 40, 169–184.
Kays, W.M., 1994. Turbulent Prandtl number. Where are we? J. Heat Transfer 116, 284–295.
Kays, W.M., Crawford, M.E., 1993. Convective Heat and Mass Transfer. McGraw-Hill, New York.
Kim, J., Mahrt, L., 1992. Simple formulation of turbulent mixing in the stable free atmosphere and nocturnal boundary layer. Tellus 44A, 381–394.
Komori, S., Ueda, H., Ogino, F., Mizushina, T., 1983. Turbulence structure in stably stratified open-channel flow. J. Fluid Mech. 130, 13–26.
Launder, B.E., Spalding, D.B., 1972. Mathematical Models of Turbulence. Academic Press, London.
Louis, J., 1979. A parametric model of vertical eddy fluxes in the atmosphere. Boundary-Layer Meteor. 17, 187–202.
Louis, J., Tiedke, M., Geleyn, J.F., 1981. A short history of the operational PBL parameterization at ECMWF. In: Workshop on Planetary Boundary Layer Parameterization. ECMWF, pp. 59–79.
Munk, W.H., Anderson, E.R., 1948. Notes on a theory of the thermocline. J. Mar. Res. 7, 276–295.
Peltier, W.R., Caulfield, C.P., 2003. Mixing efficiency in stratified shear flows. Annu. Rev. Fluid Mech. 35, 135–167.
Peters, H., Gregg, M.C., Toole, J.M., 1988. On the parameterization of equatorial turbulence. J. Geophys. Res. 93, 1199–1218.
Riley, J.J., Lelong, M.P., 2000. Fluid motions in the presence of strong stable stratification. Annu. Rev. Fluid Mech. 32, 613–657.
Rodi, W., 1993. Turbulence Models and Their Application in Hydraulics. A.A. Balkema, Rotterdam.
Strang, E.J., Fernando, H.J.S., 2001. Vertical mixing and transports through a stratified shear layer. J. Phys. Oceanogr. 31, 2026–2048.
Turner, J.S., 1973. Buoyancy Effects in Fluids. Cambridge University Press, New York/London.
Venayagamoorthy, S.K., Koseff, J.R., Ferziger, J.H., Shih, L.H., 2003. Testing of RANS Turbulence Models for Stratified Flows Based on DNS Data. Center for Turbulence Research Annual Research Briefs, pp. 127–138.
Venayagamoorthy, S.K., Stretch, D.D., 2006. Lagrangian mixing in decaying stably stratified turbulence. J. Fluid Mech. 564, 197–226.
Venayagamoorthy, S.K., Stretch, D.D., 2010. On the turbulent Prandtl number in homogeneous stably stratified turbulence. J. Fluid Mech. 644, 359–369.